

This is not a peer- reviewed paper.

Soil Stress Residuals as Indicators of Soil Compaction

Reed Turner
Project Engineer
Agricultural Technology Centre
Lethbridge, Alberta

Randy L. Raper
Agricultural Engineer
USDA-ARS National Soil Dynamics Lab
Auburn, AL

**Presented at the 2001 ASAE Annual International Meeting
Sacramento, California
July 29 - August 2, 2001**

Summary: Data from soil ground pressure sensors show that residual stress, or the net stress remaining after a vehicle has passed over the sensor, is proportional to peak stress or peak compaction force. This suggests a simple way to measure and compare soil compaction between different vehicles or treatments. This paper reviews two methods of measuring peak and residual soil stress, comparing results from a simple method to results from a more rigorous method, and reports the magnitude of the measured residual stress, and the relationships between residual stress, vehicle ground pressure and soil compactibility.

Keywords: Soil, Soil Compaction, Ground Pressure, Sensors, Measurement, Tires, Inflation Pressure, Traction, Contact Area

The author(s) is solely responsible for the content of this technical presentation. The technical presentation does not necessarily reflect the official position of ASAE, and its printing and distribution does not constitute an endorsement of views which may be expressed.

Technical presentations are not subject to the formal peer review process by ASAE editorial committees; therefore, they are not to be presented as refereed publications.

Quotation from this work should state that it is from a presentation made by (name of author) at the (listed) ASAE meeting.

EXAMPLE — From Author's Last Name, Initials. "Title of Presentation." Presented at the Date and Title of meeting, Paper No X. ASAE, 2950 Niles Road, St. Joseph, MI 49085-9659 USA.

For information about securing permission to reprint or reproduce a technical presentation, please address inquiries to ASAE.

Introduction

Soil compaction is a concern for producers and researchers. For producers, soil compaction is an economic issue because it can reduce yield. Additionally, the methods and machines used to appropriately remove or control compaction are costly and, if incorrectly applied, can provide limited or no payback. For researchers, soil compaction is a difficult parameter to quantify, particularly in real time as compaction events occur. An ideal measurement would be one from an inexpensive, easy to position sensor that showed the effect of a compaction event in real time.

The examination of data from pressure sensors inserted in the soil suggests that residual stress, or the net stress remaining after a vehicle has passed over a sensor, is closely related to the peak stress or peak compaction force, and may be used as an indicator of the compactibility and net compaction of the soil. This could be a simple way to measure and compare compaction between different vehicles and treatments. This paper will discuss two methods of measuring peak and residual stress, compare results from a simple method to results from a more rigorous method, and report the magnitude of the measured residual stresses and their relationship to the peak stresses and the vehicle actions that produce them.

Literature Review

Soil compaction is the volume decrease, density increase and structural change of soil under pressure and is a concern for farmers, agricultural equipment manufacturers and agricultural researchers. As the equipment industry has reacted to buyer demands for higher capacity equipment, the loads, pressures and working forces applied to soil have continued to increase. Studies have shown the relationship between increased compaction and the increased soil loading resulting from larger machinery (Bedard et al. 1997, Abu-Hamdeh et al. 1995, Wood et al. 1990).

Several researchers suggest that "shallow" soil compaction, that in the top 250 mm (6 in) layer, is most related to surface contact pressures from machinery while "deep" soil compaction is most related to total axle loads from machinery (Smith and Dickson, 1988). Other researchers suggest that the cumulative soil compaction effect from multiple passes by a machine is very dependent on soil initial conditions (Soane et al, 1981).

Various parameters have been measured in attempts to quantify soil compaction. In most cases, the parameters measured are soil properties that change with soil compaction. Quantifying compaction with soil property parameters requires a "before the event" and an "after the event" measurement to establish whether there has been a change in the property that would indicate a change in soil compaction.

Several descriptive soil compaction parameters are currently in common use. Cone index or penetration strength is measured directly using one of the various forms of penetrometers. Dry bulk density is measured directly using various physical core sampling methods (Erbach, 1997) or indirectly using various neutron emitting probes (Wells and Luo, 1992, Erbach, *ibid*). Moisture content is measured directly using physical sampling followed by oven drying or indirectly using various radiation methods such as Time Domain Reflectometry (Erbach *ibid*). Air filled porosity is calculated indirectly using the change in pressure when a sample is exposed to a fixed volume of gas at a known pressure (Holmes et al, 1988). Work has also been done to measure porosity directly using Computer Assisted Tomography or CAT scanning (Perret et al, 1996). Air permeability is measured directly using air permeometers which are instruments which control

pressure drop and measure air mass flow rate through standard samples (Jansson and Johansson, 1998). Efforts have been made to automate and speed up the various measurements through the use of complex portable laboratory systems (Holmes et al, 1988). The development and use of a device that performs an automatic continuous measurement of soil air permeability has been reported by Clement and Stombaugh (2000).

Various methods of measuring some aspect of pressure on or in the soil have been developed. This follows early hypotheses by Soehne (1958) that bulk density is a function of the largest principal stress in soil. VandenBerg (1958) proposed that bulk density is a function of mean normal stress which is the average of the three principal stresses. Complete three dimensional stress state maps have been measured using a combination of six directional pressure sensors mounted to a single block of material (Nichols et al, 1987, Harris and Baker, 1993). Strain gauged thin aluminum disks placed in prepared beds of sand have been used to measure vertical stresses under vehicles (Blunden et al, 1992). Carrier et al, 1995, detail the development of an "in the soil" surface pressure gauge, an elongated fluid filled rubber bladder covered with a steel partial shell and connected to a pressure transducer. All these devices require a time consuming precision placement process to control location and soil effect variability. Turner et al, 2001, used fluid filled bulbs connected to pressure transducers to obtain the pressure maximums and developed a rapid placement procedure to increase the sample rate. Other researchers have eliminated the placement process by using pressure transducer combinations mounted directly on or in tire or track surfaces (Degirmencioglu et al, 1997, Smith et al, 1994). These devices measure the pressures exerted on the soil surface.

Sensor Descriptions

Pressure in the soil is a parameter that can be measured in real time and used as an indicator of the severity and effect of a compaction event. This paper presents an analysis of peak and residual pressure measurements from two different soil pressure measurement transducers, each with its own insertion procedure.

The AgTech Ground Pressure Sensor

The AgTech sensor, hose and pressure transducer is shown in figure 1.



Figure 1 - Pressure Transducer Assembly

This sensor is a fluid filled 25 mm (1 in) diameter rubber bulb attached to a pressure transducer by a short high pressure hose. It is inserted in the soil in a predrilled angled hole and its location is determined and adjusted through the use of an adjustable drill fixture. The development of the sensor and usage procedure has been previously reported (Turner et al, 2001).

The AgTech sensor produces a time history trace of pressure in the soil at the bulb location. This shows the distribution or shape and timing of the pressure wave under a vehicle, the peak pressures produced in the soil, and the residual pressure remaining following the pass of a vehicle. Comparisons between different runs can be used to show the effects of the contact surface geometry (lug or carcass), vehicle type, and vehicle loads. Because the sensor is nondirectional, it shows magnitude but not the changes in the direction of stress that can occur with load or slip. Readings from the sensor are sensitive to temperature change and to placement induced stresses and it is necessary to convert measurements to relative pressure readings using the pressure measured before the run as the effective zero value.

The shape of the pressure wave time history also gives information about the effect of the vehicle traffic on the soil. Different types of vehicles have different time history shapes. Figure 2 shows a representative time history trace of the pressure 100 mm (4 in) underneath a rubber tire and Figure 3 shows a similar trace under a rubber belt track. Both tractors weighed 13,000 kg (28,600 lbs), were correctly setup and were operating at 5 kph (3 mph), pulling a load of approximately 45 kN (10,000 lbs).

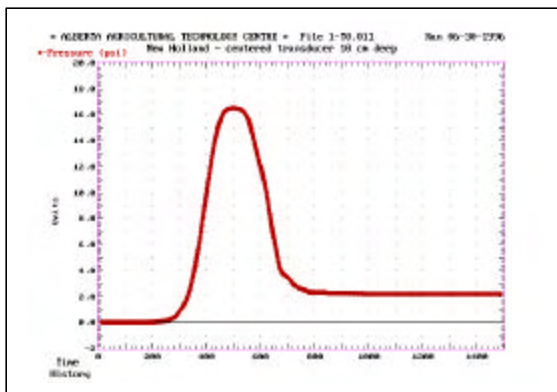


Figure 2 - Pressure under a Tire

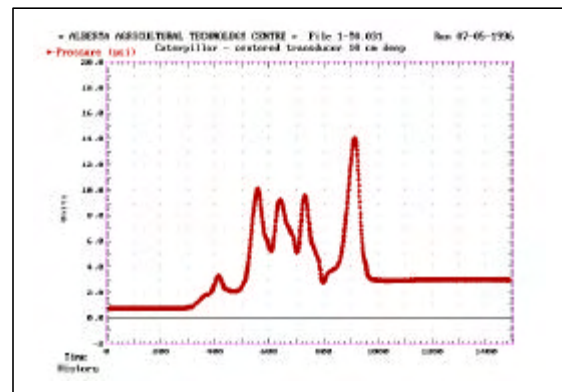


Figure 3 - Pressure under a Rubber Belt Track

The peak pressure is defined as the difference between the pressure before the vehicle approached the sensor and the highest pressure achieved as the vehicle passed over the sensor. The residual pressure is defined as the difference between the pressure before the vehicle approached the sensor and the pressure after the vehicle passed over the sensor.

Two people using the placement fixture can place, drive over and log about 40 separate readings per hour. This data rate enables statistically significant comparisons of the effects of various components and adjustments on soil pressure. Typically about 20 separate readings are made of the pressures for a given event. The peak and the residual pressures for each reading are then extracted and can be compared to those from other events using conventional statistical procedures.

The NSDL Stress State Transducer

Stress state transducers (SST's) and placement procedure have been previously described by Nichols et al. (1987). These transducers measure the pressure in six directions and provide values that allow calculations of principal stresses and octahedral normal and octahedral shearing stresses. It has been reported that a better model of soil compaction is dependent upon the entire stress state of the soil and these transducers allow this determination to be made.

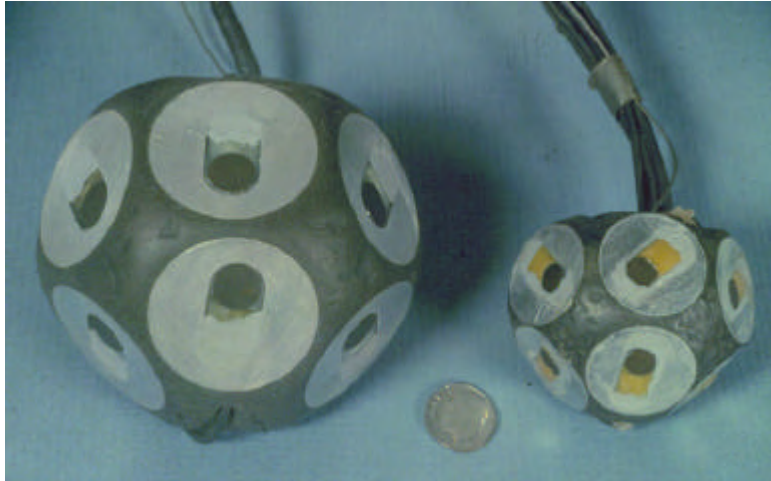


Figure 4. Typical sizes of SSTs.

SST's are typically buried in the center of the path of the tire at the depth of the hardpan or midway between a root-impeding layer and the soil surface. To bury these transducers, a hole must be excavated, usually with a post-hole digger. The transducer is then placed in the hole and the soil carefully replaced around the transducer. It requires significant time to dig the hole, place the sensor, recover it with the loosened soil, and perform the test. For a typical experiment, it took two people about 1-2 hours to prepare three sensors for a test. Four replications of each test are usually necessary for statistical significance. Therefore, any experiment that has several treatments can take several days for completion.



Figure 5 - SST being placed in hole in NSDL soil bins.

Because of the destructive nature of the placement process, measurements obtained with the SST's are usually only obtained in loosely tilled soil. Recently, however, measurements have been made using the SST to measure soil stress in soils that contain some structure.

The pressures that are measured with the SST typically show a peak when the tire is directly over the top of the transducer as shown in Figure 6 (left). Immediately after this peak is reached, the pressures quickly reduce to near their previous conditions. The pressures plotted in Figure 6 (left) show the six measured pressures which are directly measured from the SST. Figure 6 (right) shows the calculated stresses that result from determination of the stress state of the transducer. Also note in Figure 6 the residual values of stress that remain when the tire is no longer over the SST. Because the major principal stress and the octahedral normal stress have been thought to contribute the most to soil compaction (Soehne 1958; VandenBerg, 1958), their residual values will be statistically examined.

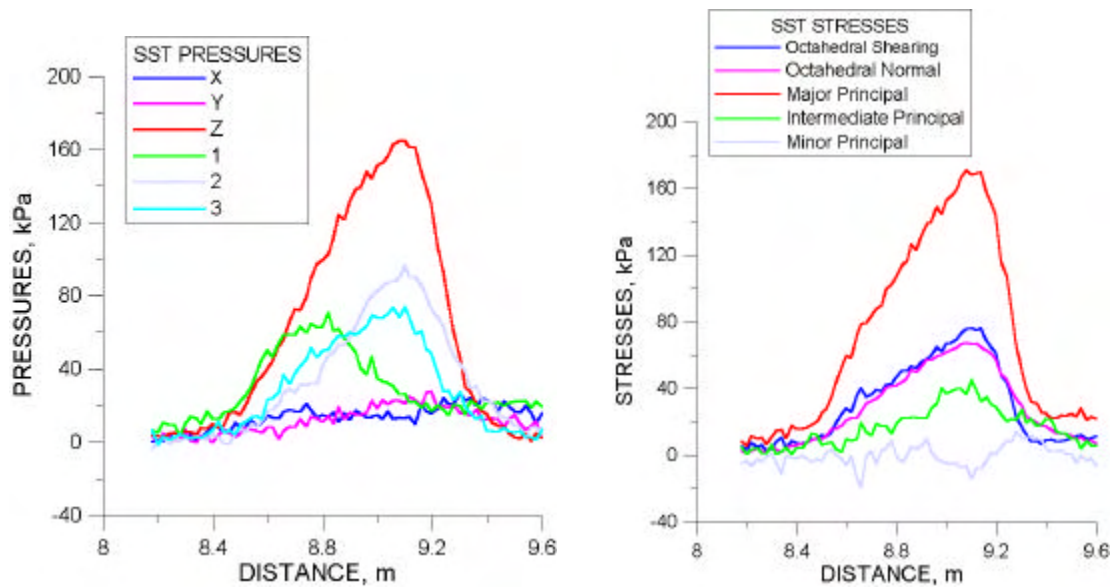


Figure 6. Pressures measured beneath the centerline of a tire with the SST (left) and then used to calculate stresses (right).

Results and Discussion - AgTech Sensor

Several series of measurements were made under two different tractors in a relatively wet (20% moisture) untilled clay loam soil. The first tractor was an MFWD rubber tire tractor, equipped with 20.8 R38 R1 radial tires on the rear, each carrying 27 kN (6000 lbs). This was equivalent to a 216 kN (48000 lbs) four wheel drive tractor equipped with eight tires. Tests were run with the tires correctly inflated to 96 kPa (14 psi) and then overinflated by 100% to 192 kPa (28 psi). The second tractor was a rubber belt tractor equipped with 915 mm (36 inch) wide belts and weighing 208 kN (46800 lbs) total, or 104 kN (23,400 lbs) per belt. Tests were run at this weight and at 121 kN (27,300 lbs) per belt, or 242 kN (54600 lbs) total for the tractor.

Measurements were made at 50 mm (2 inch), 100 mm (4 inch) and 150 mm (6 inch) depths in the soil. For each test setup a series of 10 to 12 sets of measurements were taken using two bulbs spaced in the direction of travel at 1.5 times the lug bar spacing (to maximize the probability of getting at least one bulb under a lug). The time histories were plotted and the peak and residual values were extracted. These data were then analyzed using the General Linear Model procedure in Systat to obtain the least squares means and standard error ranges and to evaluate significant effects and interactions. The Bonferroni Pairwise Mean Comparison procedure was used to determine significance or confidence levels for differences in the means. All differences in the means shown in this report are significant at greater than 99.99% probability unless they are individually reported otherwise. The graphs presented were output from the Systat software and show all mean values with error bar ranges set to indicate one standard error.

Residual versus Peak Pressure

Residual pressure correlated closely with peak pressure. Figure 7 shows regressions and 95% confidence intervals for residual pressure as a function of peak pressure at 50 mm, 100 mm and 150 mm depths under the rubber tires with both test pressures combined. Figure 8 shows the same information for the track machine with both test weights combined.

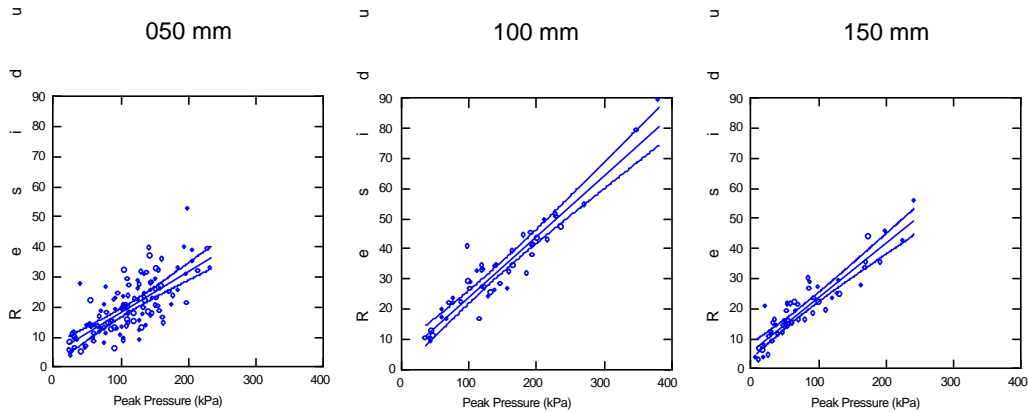


Figure 7 - Residual Pressure as Function of Peak Pressure under Rubber Tire

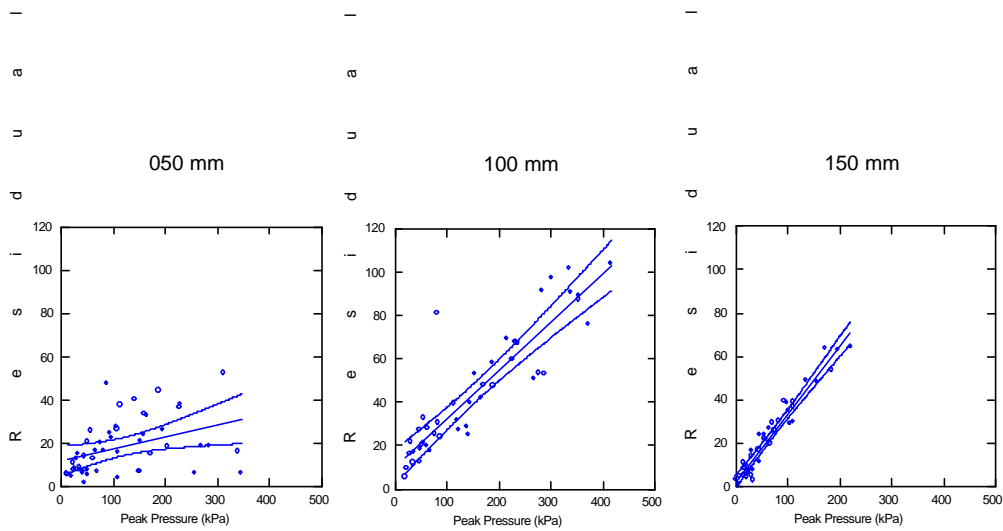


Figure 8 - Residual Pressure as Function of Peak Pressure under Rubber Belts

While all the data showed excellent correlation, the 50 mm data are more scattered. This appeared to be due to the soil near the surface fracturing after the vehicle passed by and effectively "releasing" the pressure bulb. This was particularly true when the bulb happened to be directly under a lug. When this happened, the soil layer remaining between the bulb and the lug surface after the pass was typically only 12 to 25 mm (.5 to 1 inch) thick and would often hump up or crack directly over the bulb after the lug had passed. The soil effectively did not have enough cohesive strength or clumping force to retain the pressure around the bulb.

Effect of Traction System Type

As shown in Figure 2 and 3, the time histories of pressure under the rubber tire and rubber belt were quite different. As shown in Figure 9 and 10, the peak and residual pressures under the rubber belt machine fell between those under the overinflated rubber tire and the correctly inflated tire.

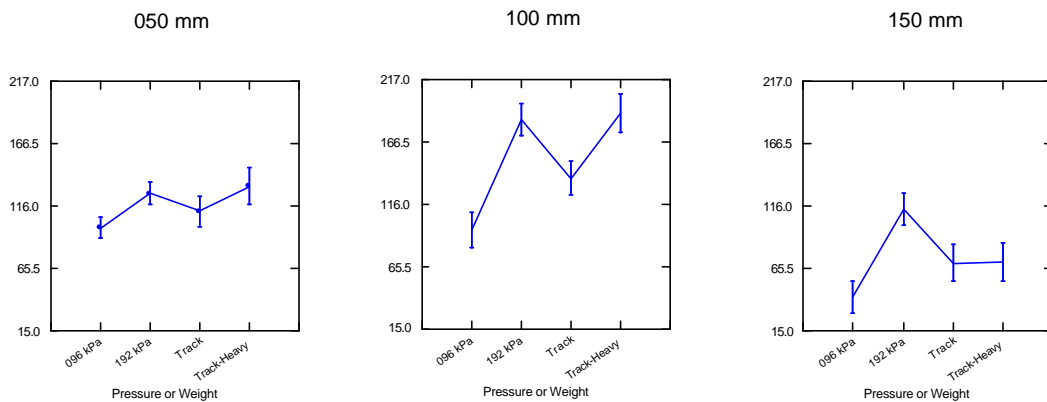


Figure 9- Peak Pressures under the Tires and Rubber Belts.

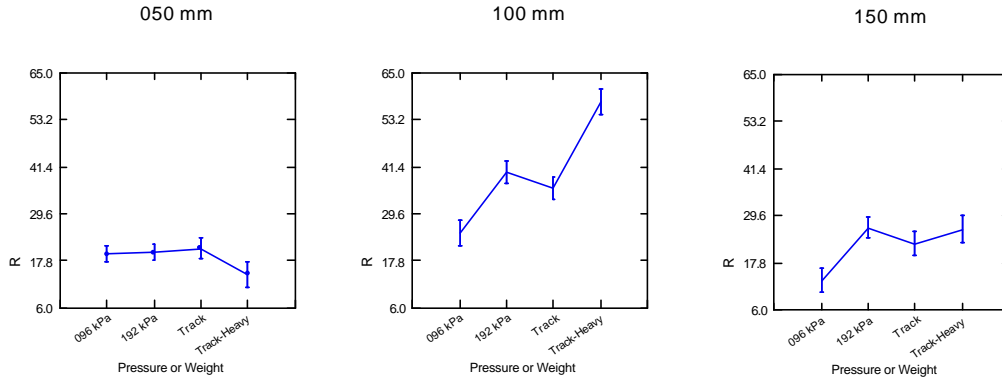


Figure 10 - Residual Pressures under the Tires and Rubber Belts.

Mean differences for the residual pressures and the associated probabilities are shown in Table 1. The data shows a high probability that the low pressure tire has a lower residual pressure than the other configurations at the 100 and 150 mm depth.

Table 1 Residual Pressure Mean Differences and Probabilities

Differences in the Residual Pressure Means											
	050 mm				100 mm				150 mm		
	96 kPa	192 kPa	Track		96 kPa	192 kPa	Track		96 kPa	192 kPa	Track
96 kPa	0.00				0.00				0.00		
192 kPa	0.45	0.00			15.13	0.00			13.22	0.00	
Track	1.35	0.91	0.00		11.29	-3.84	0.00		9.19	-4.03	0.00
Track-Heavy	-5.11	-5.56	6.47		32.96	17.83	21.67		12.69	-0.53	3.50
Bonferroni Adjusted Probabilities that Means are Different											
	050 mm				100 mm				150 mm		
	96 kPa	192 kPa	Track		96 kPa	192 kPa	Track		96 kPa	192 kPa	Track
96 kPa	-				-				-		
192 kPa	0.0%	-			91.7%	-			99.6%	-	
Track	0.0%	0.0%	-		61.4%	0.0%	-		85.5%	0.0%	-
Track-Heavy	65.2%	76.6%	80.6%		100.0%	97.0%	100.0%		97.8%	0.0%	0.0%

Additionally, as can be seen in Figure 7 and 8 and in the standard error range sizes in Figure 9 and 10, there was greater variation in the readings taken under the rubber belts. This may be attributable to pressure differences across the width of the rubber belt. While the tire load was carried on a cushion of air which tended to distribute the load equally across the inner surface of the tire, this was not true for the belt. Across the width of the belt, some of the belt was in direct contact with load carrying rollers and some was not, as figure 11 shows. Sensor placement variations across the belt width were not as well accounted for as they were along the length and this may have contributed to the greater data scatter under the belts.

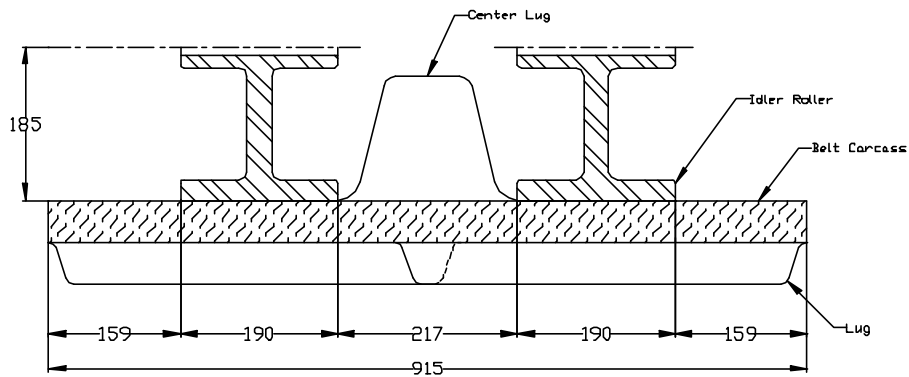


Figure 11 - Rubber Belt Machine Component Cross Section - One Belt

Effect of Depth

Both peak and residual pressures decreased as depth increased beyond 100mm. The magnitude of the changes with depth were similar for the rubber tire and the rubber belt. Figure 12 shows the rubber tire pressures vs depth and figure 13 shows the same for the rubber belt. The increase in pressure exhibited between 50 mm and 100 mm is difficult to explain but was repeatable. It may have been related to the finite size of the 25 mm (1 inch) diameter measurement bulb. All depth measurements are given from the soil surface to the center of the sensor bulb.

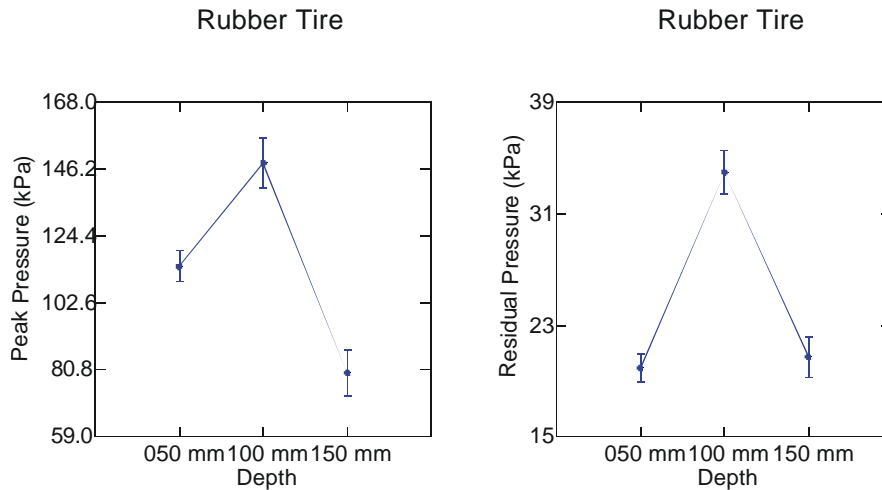


Figure 12 - Pressure Changes with Depth for the Rubber Tire

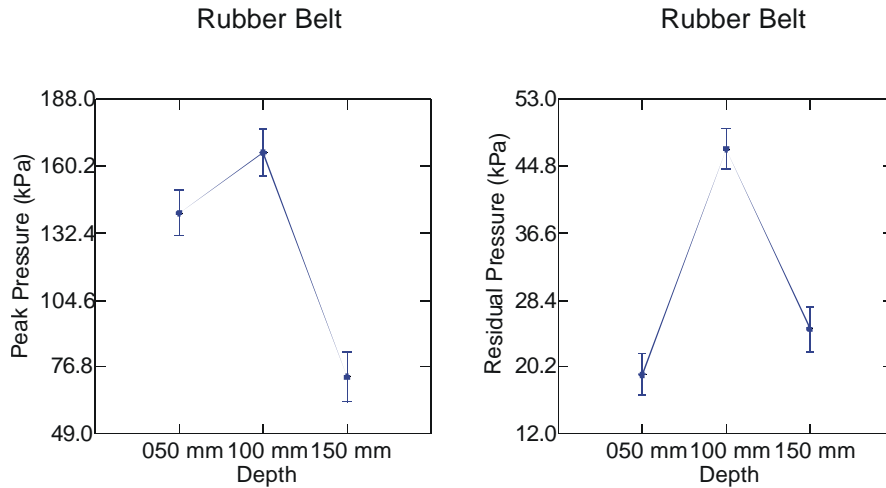


Figure 13 - Pressure Change with Depth for the Rubber Belt

Effect of Tire Inflation Pressure

As figure 14 shows, peak and residual pressure were closely related to inflation pressure for the tire. As figure 9 shows, the peak pressures at the 100 mm depth were approximately equal to the inflation pressure of the tires.

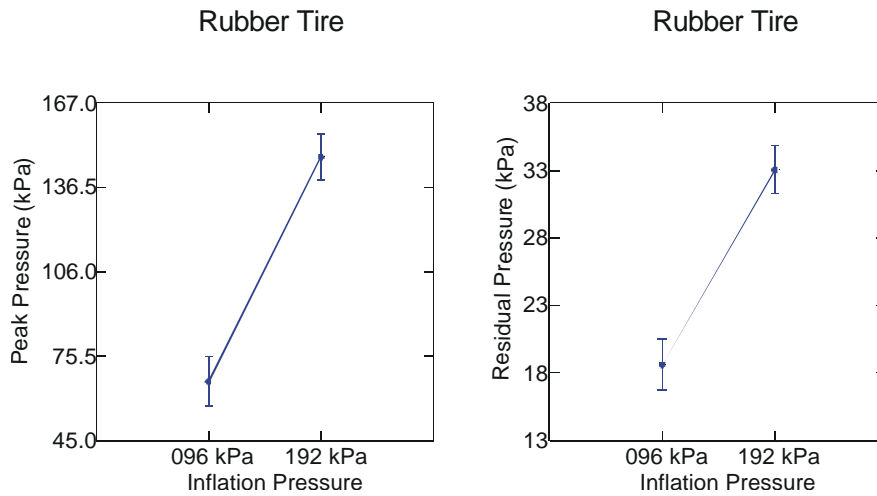


Figure 14 - Pressure Change with Inflation Pressure for the Rubber Tire

Effect of Weight on the Rubber Belt

Although the different weights tested for the rubber belt represented only a 17% increase, the sensor pressure readings increased with the additional weight, as figure 15 shows. The significance levels for the differences were lower, only 85% for the peak pressure and 89% for the residual pressure.

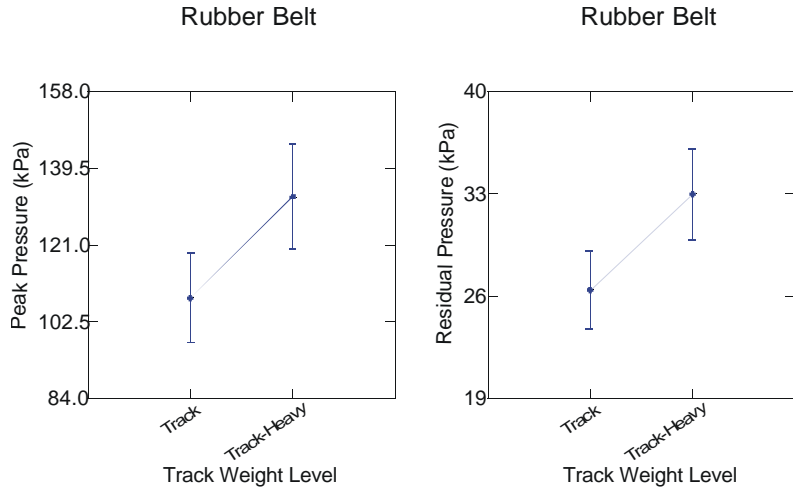


Figure 15 - Pressure Change with Weight Change for the Rubber Belt

Effect of Contact Area Geometry

The geometry of the contact surface affected readings at all depths tested. To measure this, readings were made at zero slip so that the contacting surface above the sensor remained constant as the vehicle moved over the sensor. After each run the tread imprint and sensor location were noted to determine whether carcass or lug had been directly over the sensor. Tests where the sensor was on an edge, carcass to lug or lug to carcass, were placed in a third category, called edge. Figure 16 shows this location data for the rubber tire and Figure 17 shows similar data for the rubber belt. As can be seen, pressures under the lug were significantly higher than pressures under the carcass. As shown in Figure 18 and 19, this was true at all depths tested except for the tire at 150 mm (6 inches). For the tire, the "on edge" readings were not significantly different from the "under carcass" readings at any of the depths.

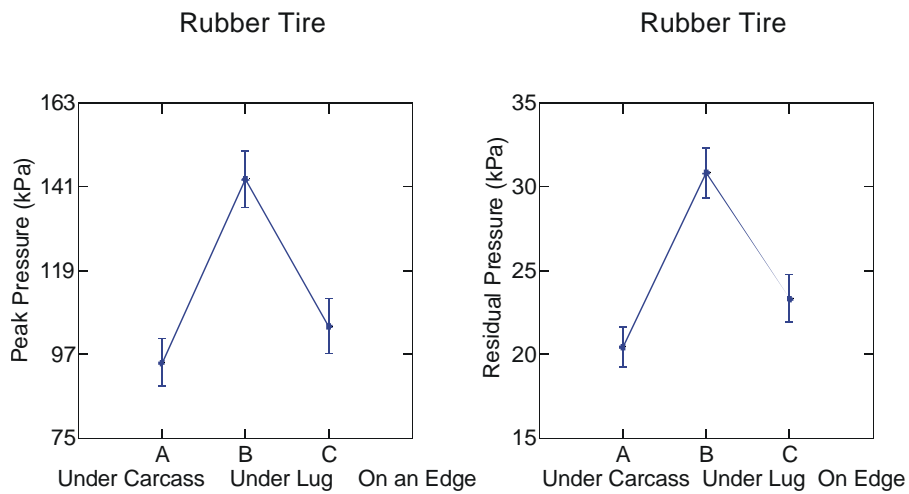


Figure 16 - Pressure Changes with Contact Surface Location for Rubber Tire

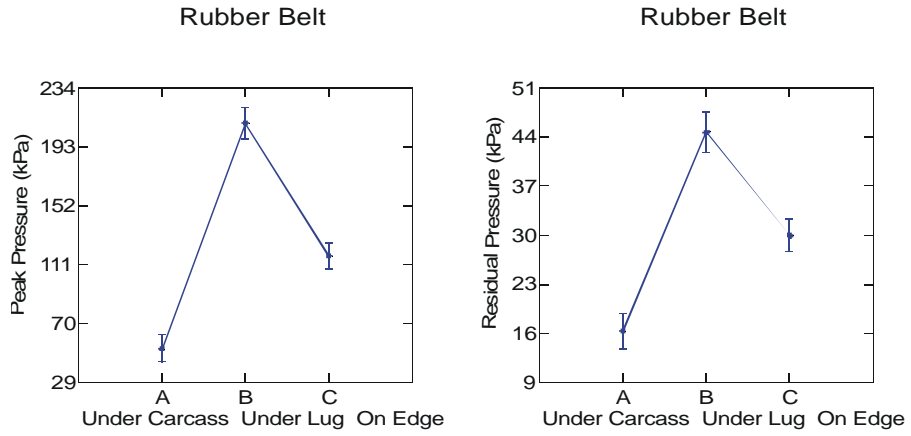


Figure 17 - Pressure Changes with Contact Surface Location for Rubber Belt

Rubber Tire

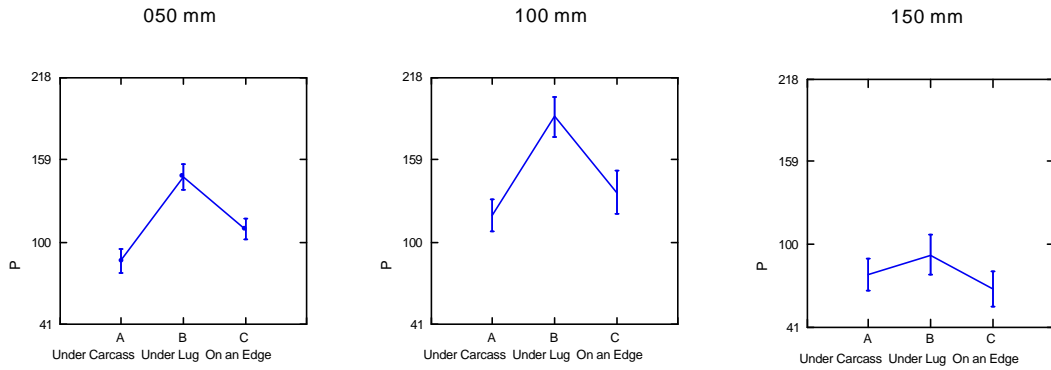


Figure 18 - Pressure Changes under the Tire as affected by Depth and Contact Location

Rubber Belt

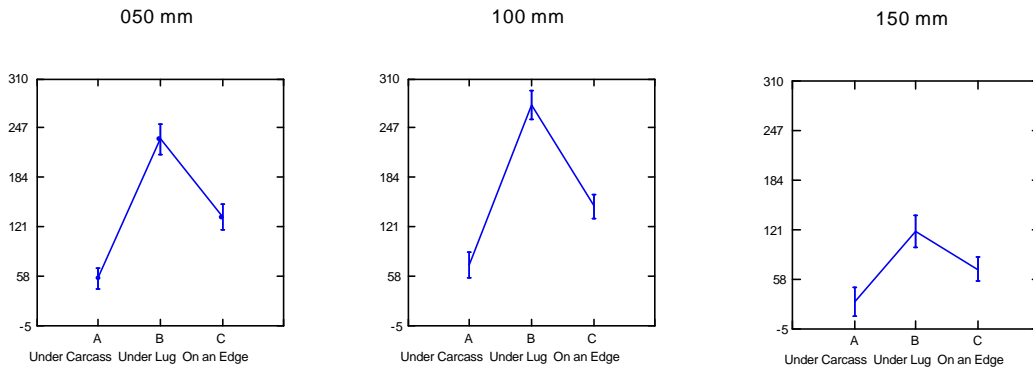


Figure 19 - Pressure Changes under the Belt as affected by Depth and Contact Location

Results and Discussion - NSDL Sensor

To evaluate the ability of the SST to measure the residual stresses after the tire has passed over the transducers, stress data obtained from a previous compaction experiment were examined. That experiment was conducted in the soil bins at the USDA-ARS National Soil Dynamics Laboratory in Auburn, Alabama to investigate the effect of inflation pressure and dynamic load on tire and soil parameters. Soils chosen for the study were a Norfolk sandy loam soil (*Typic Paleudults*) and a Decatur clay loam soil (*Rodic Paleudults*). Both soils were from the Southeastern United States and they contained a wide range of particle size distributions. These soils were selected because they are located indoors which facilitates the maintenance of a constant moisture content for an extended period of time.

Two soil conditions were created in each soil bin to give a different operating environment for the tire. A hardpan condition was created in each soil bin to simulate a condition that is commonly found in the Southeastern United States in Coastal Plains areas. This hardpan is usually 0.2 to 0.3 m below the soil surface and it is quite impervious to root growth, particularly at low moisture levels. Variations can occur between bins, but within a bin the same depth of the hardpan can usually be achieved with little error. For the Norfolk sandy loam soil, the hardpan depth established was at 0.41 m and for the Decatur clay loam soil, the hardpan depth established was at 0.29 m. The other soil condition was a uniformly loose condition which was created by operating a rototiller to a depth of approximately 0.6 m.

Table 2. Soil measurements showing the initial soil condition of the two indoor soil bins at the NSDL used for this experiment.

Depth (cm)	Bulk Density (Mg/m ³)	Moisture Content (%db)	Cone Index (MPa)
Norfolk sandy loam soil (Sand 72%, Silt 17%, Clay 11%)			
Hard Pan			
1 - 5	1.18	6.4	0.17
36-40	1.32	7.1	0.72
42-46	1.89	7.8	6.03
Uniformly Loose			
1 - 5	1.24	7.6	0.14
32-36	1.19	7.7	0.94
40-44	1.19	7.6	1.10
Decatur clay loam soil (Sand 27%, Silt 43%, Clay 30%)			
Hard Pan			
1 - 5	1.06	11.7	0.14
24-28	1.10	12.9	0.98
30-34	1.81	15.2	3.82
Uniformly Loose			
1 - 5	1.16	14.6	0.16
25-29	1.08	13.4	1.26
31-35	1.15	13.3	1.54

The tire used for the experiment was a Goodyear¹ 18.4 R38 Dyna Torque Radial (2 star) R-1 agricultural tractor tire. This tire was mounted on the Traction Research Vehicle which has the capability of controlling dynamic load, inflation pressure, slip, and input torque as described by Burt et al. (1980) and Lyne et al. (1983). For this experiment a constant slip value of 10% and a constant forward velocity of 0.15 m/s was chosen.

¹ The use of company names or tradenames does not imply endorsement.

Five combinations of inflation pressure and dynamic load were used for this randomized complete block experiment. A **HIGH** load condition of 25.3 kN dynamic load and 124 kPa inflation pressure, a **MEDIUM** load condition of 19.8 kN dynamic load and 82 kPa inflation pressure, and a **LOW** load condition of 13.2 kN dynamic load and 41 kPa inflation pressure come directly from the dynamic load-inflation pressure tables supplied from the tire manufacturer (Goodyear, 1992). An **OVERLOAD** load condition of 25.3 kN dynamic load and 41 kPa inflation pressure represent an overloaded tire condition which should not be practiced by farmers but is useful for experimental purposes. An **UNDERLOAD** load condition of 13.1 kN dynamic load and 124 kPa inflation pressure load condition represents a tire condition with excessive inflation pressure for the load. However, the **UNDERLOAD** load condition is a typical scenario found on farms throughout the United States. Four replications of these loads were conducted in each soil bin in each soil condition.

Three stress state transducers (SST) were placed beneath the center of the tire to measure the soil stress. Two SST's were identical in appearance (C and D) and differed only in their depth of placement. SST C was placed immediately above the hardpan or at the same depth if no hardpan was present. The top of SST C was approximately 355 mm below the loose surface of the Norfolk sandy loam soil and 245 mm below the surface of the Decatur clay loam soil. SST D was placed between the surface and SST C at a shallower depth of 260 mm in the Norfolk soil and 210 mm in the Decatur soil. A third SST, G, differing in appearance from the other SST's because of a newer construction method and slightly different size was placed at the same depth at SST C. A complete analysis of SST C and D peak values was reported by Bailey et al. (1993). Cone index values were obtained from the center of the tire track after the treatments had been applied.

The residual stresses were first plotted vs. the peak stresses measured with the individual SST's across all soil types and soil conditions. Slightly better fits were obtained for SST G at the shallower depths, therefore graphs from this transducer will be used to demonstrate comparisons with residual pressures. As can be seen from Figures 20 and 21 for mean normal stress and major principal stress, a great amount of scatter is found with these measurements. The peak mean normal stress has an average value of 57 kPa while the residual mean normal stress has an average value of only 8 kPa (Figure 20). This lesser value is so near the bottom of the feasible measurement spectrum with the SST that these values have little meaning. A slightly upward trend was found with increased peak mean normal stress values resulting in increased residual mean normal stress, but the fit was poor with a correlation coefficient of only 0.10. Slightly more success was obtained by plotting peak major principal stress vs. the residual major principal stress (Figure 21). The average value of peak major principal stress was 140 kPa while the average value of residual major principal stress was 17 kPa. Again, a great amount of scatter was found with the data, but the slightly upward trend is obvious with a slightly higher correlation coefficient of 0.20.

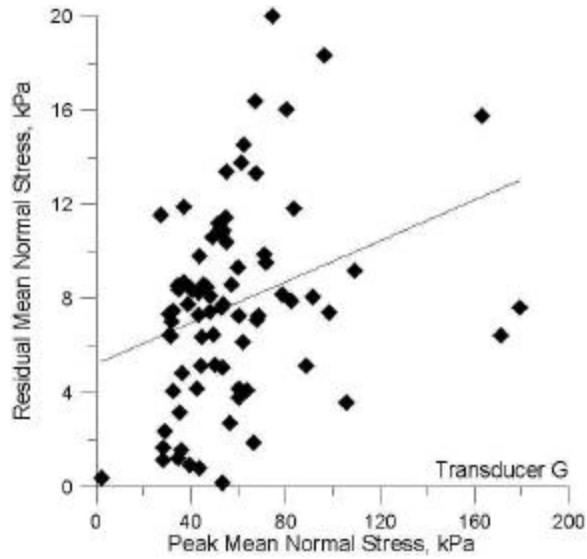


Figure 20. Residual vs. peak stresses for mean normal stress for SST G.

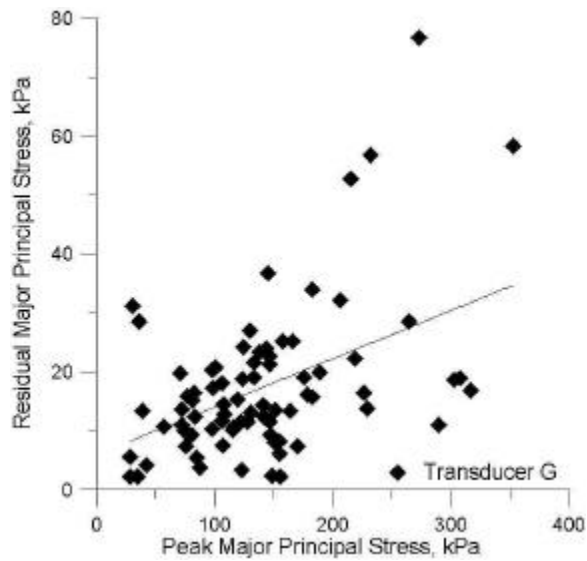


Figure 21. Residual vs. peak stresses for major principal stress for SST G.

The peak stresses and residual stresses were then plotted versus the increased cone index values caused by the tire treatments (Figures 22 and 23). The increased cone index values were obtained by subtracting the initial values of cone index from the final values obtained after the tire treatments had been applied. Slightly better agreement was found for the major principal stresses, probably because of their greater numerical size, as compared to the mean normal stress. Values obtained from SST G are shown because they are indicative of the other SST's. All of these graphs showed a great deal of scatter with poor correlation coefficients being obtained in each case.

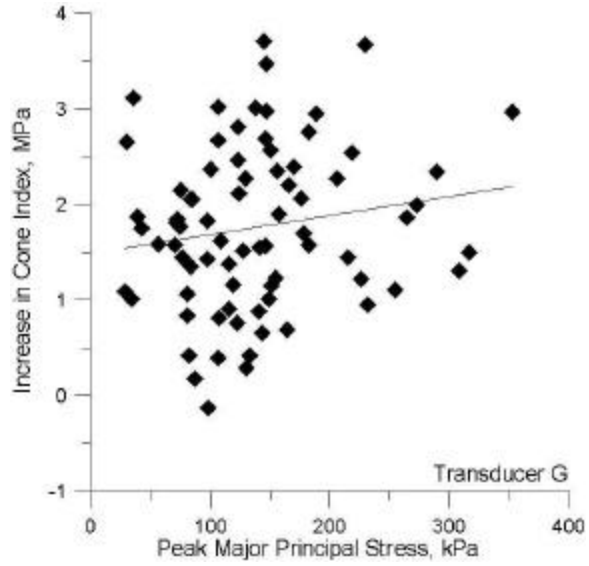


Figure 22. Increase in cone index versus peak major principal stress for SST G.

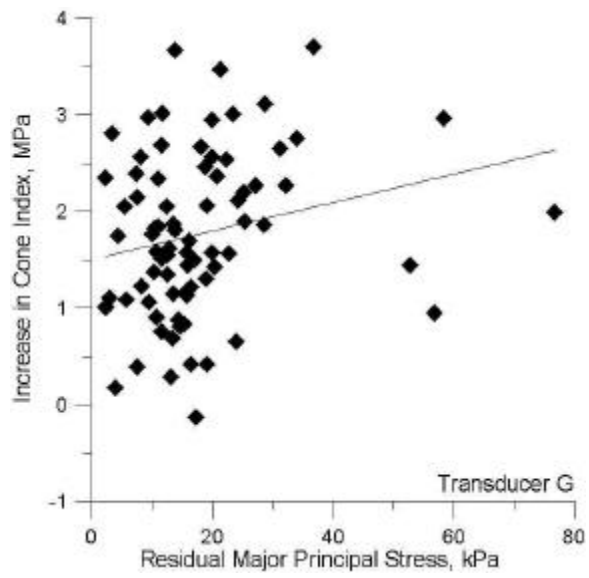


Figure 23. Increase in cone index versus residual major principal stress for SST G.

Figure 24 shows the residual stresses remaining for the mean normal stress. As can be seen from the graph and the previous discussion, these stress values are very small and rarely exceed 20 kPa. Partly because of these small values, statistical significance is difficult to achieve and differences between treatments are not always found. In the Norfolk hard pan soil condition, the **OVERLOAD** treatment was found to create residual stresses of SST D significantly below all other treatments. In the Norfolk loose soil condition, SST C showed that the **LOW** treatment created significantly reduced residual stresses. Contrary to the hardpan soil condition, SST D showed increased levels of residual stress for the **OVERLOAD** treatment. In the Decatur hardpan soil condition, the **HIGH** treatment showed increased values of residual stress.

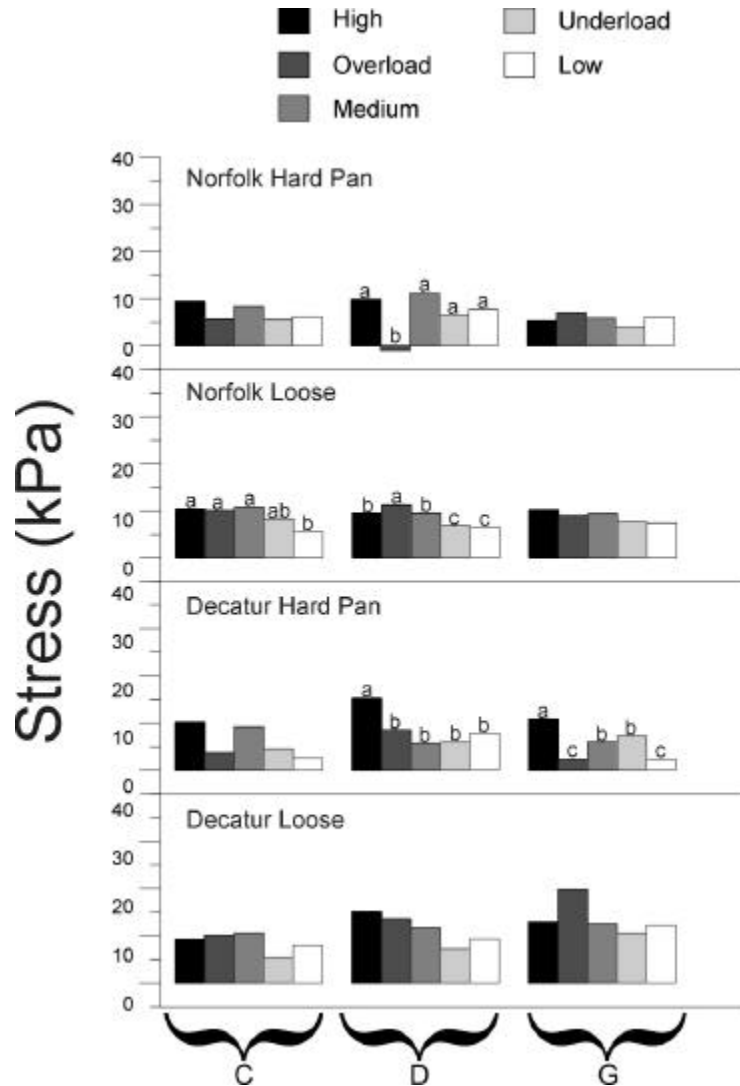


Figure 24. Residual mean normal stress from two soil types and two soil conditions remaining after load was removed. C, D, and G refer to three soil stress state cells located under the center of the tire.

Figure 25 shows the residual stresses resulting from the major principal stress measurements with the SST's. The Norfolk hardpan soil condition mostly shows the increased levels of residual stress that results from the **HIGH** treatment. The **OVERLOAD** treatment shows greatly reduced residual stresses for all three SSTs. In the Norfolk loose soil condition, the **LOW** treatment shows significantly reduced residual stresses as compared to the other treatments. The Decatur hardpan soil condition shows clear differences in residual stresses between the **HIGH** and **OVERLOAD** treatments for all three SSTs.

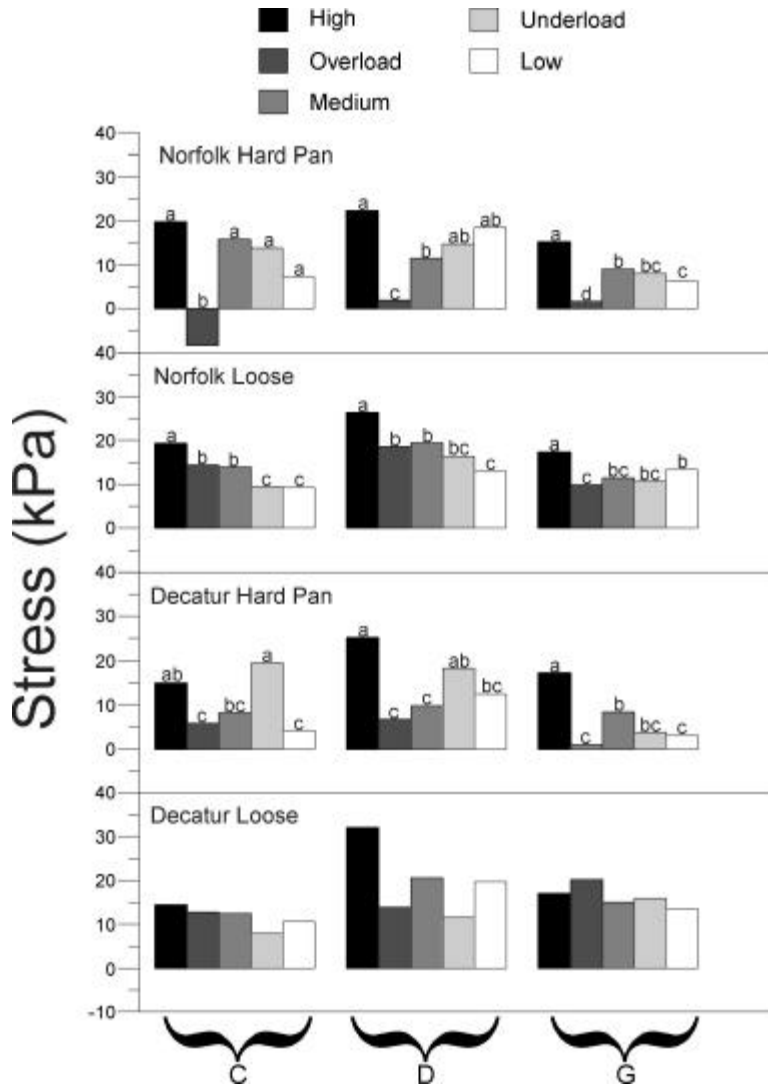


Figure 25. Residual major principal stress from two soil types and two soil conditions remaining after load was removed. C, D, and G refer to three soil stress state cells located under the center of the tire.

Some general trends concerning the tire treatments can be obtained from examining Figures 24 and 25. Despite exerting similar dynamic loads on the soil as with the **HIGH** and **OVERLOAD** treatments, benefits can be obtained by reducing inflation pressure in tires. In most soil conditions, similar residual stresses are found with the **OVERLOAD** treatment as with the **LOW** treatment which has a much smaller dynamic load applied.

Conclusions

It is possible to measure peak and residual stresses in real time in soil undergoing compaction.

Residual stresses in soil are proportional to peak stresses produced by compaction events.

Peak and residual stresses in soil are affected by contact area geometry to depths greater than 150 mm (6 inches) and are substantially higher under lugs or projections in the contact surface.

Theoretical average ground pressure is a very poor descriptor of actual pressures under a ground contact surface, especially those not relying on a suspending cushion of air to provide uniform force on the upper surface of the ground contact surface.

Overinflated radial tires show higher peak and residual stresses than correctly inflated radial tires.

Correctly inflated radial tires show lower peak and residual stresses than rubber belts carrying similar tractor weights.

Pressures under rubber belts show higher variance with position than those under rubber tires.

There is significantly more scatter when using SST's to measure residual stresses as compared to the AgTech sensor. This may be due to the greater structural rigidity of the SST when compared to sensors which are able to deform slightly under load.

References

- Abu-Hamdeh, N., R.K. Wood, T.G. Carpenter, R.G. Holmes. 1995. Soil Physical Response to Various Tire and Track Systems. ASAE Paper No. AETC 95032. St. Joseph, MI: ASAE.
- Bailey, A.C., R.L. Raper, T.R. Way, E.C. Burt, and C.E. Johnson. 1996. Soil stresses under a tractor tire at various loads and inflation pressures. *J. Terramechanics* 33(1)
- Bedard, Y., S. Tessier, C. Lague, Y. Chen 1997. Soil Compaction by Manure Spreaders Equipped with Standard and Oversized Tires and Multiple Axles. *Transactions of the ASAE* 40(1):37-43.
- Blunden, B.G., C.B. McLachlan, J.M. Kirby. 1992. Technical Note: A Method of Measuring in Situ Soil Stresses Due to Traffic. *Soil and Tillage Research* 25:35-42.
- Burt, E.C., C.A. Reaves, A.C. Bailey, and W.D. Pickering. 1980. A machine for testing tractor tires in soil bins. *Trans. of ASAE* 23(3):546-547, 552.
- Carrier, D., S. Tessier, L. Chi, N.B. McLaughlin. 1995. Soil Ground Pressure Distribution Device. CSAE Paper No. 95-401. Saskatoon, SK.: CSAE.
- Clement, B.R., and T.S. Stombaugh. 2000. Continuously-Measuring Soil Compaction Sensor Development. ASAE Paper No. 001041. St. Joseph, MI: ASAE.
- Degirmencioglu, A., R.H. Wilkinson, A.K. Srivastava, T.H. Wolff, T.R. Way. 1997. Effects of Dynamic Load, Inflation Pressure and Slip on Soil-Tire Interface Pressures. ASAE Paper No. 97-1024. St. Joseph, MI: ASAE.

- Erbach, D.C., 1987. Measurement of Soil Bulk Density and Moisture. *Transactions of the ASAE* 30(4):922-931.
- Goodyear. 1992. Optimum tractor tire performance handbook. The Goodyear Tire & Rubber Company. January.
- Harris, H.D., and D.M. Bakker. 1994. A Soil Stress Transducer for Measuring In Situ Soil Stresses. *Soil and Tillage Research* 29(1994):35-48.
- Holmes, R.G., M.T. Morgan, T.G. Carpenter, T. Nau 1988. Automated Soil Core Sampler and Soil Physical Properties Measurement. ASAE Paper No. 88-1631. St. Joseph, MI: ASAE.
- Jansson, K.J., and J. Johansson. 1998. Soil Changes After Traffic With a Tracked and Wheeled Forest Machine: A Case Study on a Silt Loam in Sweden. *Forestry* 71(1):57-66.
- Lyne, P.W.L., E.C. Burt, and J.D. Jarrell. 1983. Computer control for the National Tillage Machinery Laboratory single-wheel tester. ASAE Paper No. 83-1555, ASAE, St. Joseph, MI 49085.
- Nichols, T.A., A.C. Bailey, C.E. Johnson, R.D. Grisso. 1987. A Stress State Transducer for Soil. *Transactions of the ASAE* 30(5):1237-1241.
- Perret, J.S., H. Pizarro, S.O. Prasher, A. Kantzas, C. Langford. 1996. Imaging and Analysis of the Pore Structure of Undisturbed Soil Columns by X-Ray Computed Tomography. CSAE Paper No. 96-109. Saskatoon, SK.: CSAE.
- Shi, Y.L., D. Wulfsohn, R.J. Ford, E. Richardson. 1996. Soil Compaction by Timber Harvesting System in Central Saskatchewan. CSAE Paper No. 96-405. Saskatoon, SK.: CSAE.
- Smith, B.E., T.N. Burcham, F.S. To, K.W. VanDevender, R.K. Matthes. 1994. Mobile Soil-Tire Interface Measurement System. *Transactions of the ASAE* 37(5):1633-1637.
- Smith, D.L. and J.W. Dickson. 1990. Contributions to Vehicle Weight and Ground Pressure to Soil Compaction. *Journal of Agricultural Engineering Research* (1990)46:13-29.
- Soehne, W. H. 1958 Fundamentals of pressure distribution and compaction under tractor tires. *Agricultural Engineering* 39(5):276-281.
- Turner, R.J., K. Schmidt. M. Fournier, K. Lepage. 2001. Development of a Simple System for Measuring Peak Soil Stresses. ASAE Paper No. 01AETC03. St. Joseph, MI: ASAE.
- VandenBerg, G.E., W.F. Buchele, and L.E. Malvern. 1958. Application of continuum mechanics to soil compaction. *Trans. ASAE* 1(1):24-28.
- Wells, L.G., and X. Luo. 1992. Evaluation of Gamma Ray Attenuation for Measuring Soil Bulk Density Part II: Field Evaluation. *Transactions of the ASAE* 35(1):27-32.
- Wood, R.L., M.T. Morgan, R.G. Holmes, K.N. Brodbeck, T.G. Carpenter, R.C. Reeder. 1990. Soil Physical Properties as Affected by Traffic: Single, Dual and Flotation Tires. ASAE Paper No. 90-1550. St. Joseph, MI: ASAE.